

Review

# Martensite

Druce Dunne 

Faculty of Engineering and Information Science, University of Wollongong, Wollongong, NSW 2522, Australia; druce@uow.edu.au; Tel.: +61-2-4221-4196

Received: 27 April 2018; Accepted: 21 May 2018; Published: 29 May 2018



**Abstract:** Martensite and martensitic transformations in metals and alloys have been intensively studied for more than a century and many comprehensive and informative reviews have been published. The current review differs insofar as the analysis is performed largely through the prism of detailed studies of the changes in the martensitic transformation in Fe<sub>3</sub>Pt alloy as a result of austenite ordering. This important alloy is the first ferrous alloy identified as exhibiting thermoelastic transformation and shape memory. The effect of parent phase order on the martensitic transformation offers significant insights into general understanding of the nature of martensitic transformation, particularly the factors contributing to reversible and irreversible transformation. It is concluded that for crystallographically reversible transformation to occur both strain limiting and strain accommodating factors must be present and that these factors collectively constitute the sufficient condition for reversible martensitic transformation. Although the crystallography of individual plates formed in a given alloy can change with their temperature of formation, this intrinsic variability has not been considered in analyses using phenomenological theory. Significant variability can exist in measured quantities such as habit plane normals and orientation relationships used to test theoretical predictions. Measured lattice parameters, essential data for theoretical calculations, can also differ from the actual parameters existing at the temperature of plate formation.

**Keywords:** martensite; martensitic transformation; steels; Cu-based alloys; Ti-Ni-based alloys; Fe-Pt alloys; reversible martensitic transformation; shape memory

## 1. Introduction

The use of the term “martensite” to describe the hard microstructure produced by quenching of medium and high carbon steels was coined by Osmond [1] in honour of Professor Adolf Martens who had conducted intensive metallographic research on the microstructures of steels over two decades beginning in the year 1878. Martens could not have foreseen how his observation of the plate-like phase in quenched steels would immortalize him through the countless studies and references to “martensite” by subsequent generations of metallurgists and materials scientists. Edgar Bain achieved similar fame through the coining of the term “bainite” by his research colleagues in 1934 to describe the plate- or lath-shaped ferrite (plus carbide) constituent produced in steels by isothermal treatment or continuous cooling at an intermediate rate that prevents the formation of ferrite and/or pearlite at higher temperatures and martensite at lower temperatures [2].

Campbell in 1926 [3], followed by Greninger and Mooradian in 1938 [4], reported that microstructures produced in Cu-Al and Cu-Sn alloys had similar characteristics to the martensitic phase observed in quenched steel. Greninger and Mooradian made the prescient observation that “the term martensite will eventually transcend its original meaning and come to signify a structural type in non-ferrous alloys as well as steel”. By the early 1950s “martensite” was used to describe structures observed in low carbon steels, Ti, Zr, Co, and their alloys, as well as in Cu-Sn, Cu-Al and Au-Cd alloys. The unifying feature of a “martensitic transformation” has been aptly defined by Christian [5] by the term “military transformation”,

in which “the rearrangement of the atomic configuration takes place in an orderly, disciplined manner . . . where (in principle) none of the atoms changes place with its neighbours.” It follows that this type of transformation must be diffusionless. The characteristics of the transformation also imply that it is displacive, i.e., the formation of the martensitic phase involves displacement of a volume of the original or parent phase, which is termed “austenite” in the case of steels.

Martensite and martensitic transformations have been the focus of several excellent reviews [5,6] and books [7–10], and although the present contribution can also be regarded as a review, it has been written through the perspective of the author’s research experience which spans a period of more than four decades. This experience covers the areas of the crystallography and morphology of the transformation in steels, shape strain measurements, thermoelastic martensitic transformation, and shape memory phenomena in ferrous and non-ferrous alloys. One research area that is highlighted in this paper is thermoelastic martensitic transformation in ordered Fe-Pt alloys containing about 25 at. % Pt [11]. As well as being the first ferrous alloy identified as exhibiting thermoelastic transformation and shape memory [12], it offers significant insights into the mechanisms of reversible and irreversible martensitic transformation from the structural, crystallographic, kinetic, and thermodynamic viewpoints.

This review concentrates on the kinetics and crystallography of martensitic transformation, before considering the nature of the martensite/austenite interface and the factors that contribute to crystallographically reversible martensitic transformation and shape memory phenomena.

## 2. Kinetics of Martensitic Transformation

Martensite starts to form on cooling at a characteristic temperature ( $M_s$ ) which is a function of alloy composition and the grain size and thermomechanical state of the parent (austenite) phase. Externally applied stress and/or magnetic fields can also affect  $M_s$  [7,9]. The finish temperature ( $M_f$ ) is usually less well-defined as complete transformation to martensite is approached asymptotically and small amounts of residual austenite can be retained. The corresponding temperatures for reverse transformation to austenite are  $A_s$  and  $A_f$ .

Three kinetic modes of martensitic transformation, shown schematically in Figure 1, have been identified: athermal, burst, and isothermal [13]. Many alloys, especially ferrous alloys, exhibit athermal kinetics for which the amount of martensite formed is a function of the temperature to which the alloy has been cooled and not to the holding time at that temperature, see Figure 1a. It is generally assumed that, provided the cooling rate exceeds the critical rate required to suppress any diffusional transformation, the martensitic transformation is independent of cooling rate. However, it has been observed that the transformation can be influenced by cooling rate, at least for steels, because of dynamic thermal stabilization of austenite [14]. Static thermal stabilization is observed on arresting the cooling process and holding at the quench temperature. On subsequent re-cooling, a temperature decrement ( $\Delta T$ ) is required before martensite formation restarts. This phenomenon is called thermal stabilization and is considered, in the case of C-bearing steels, to be due to C segregation to dislocation substructures in the remnant austenite that attenuates their potency as nucleation sites [13].

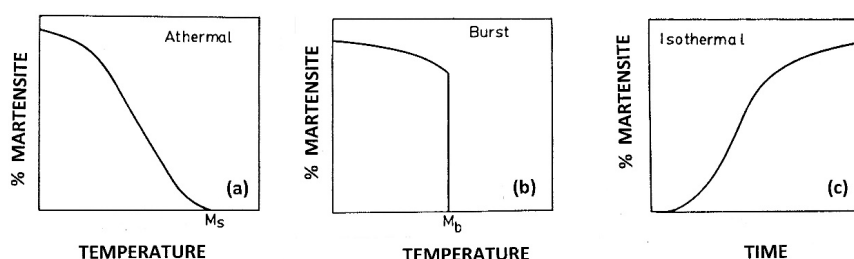


**Figure 1.** Schematic diagrams showing the three kinetic modes of martensitic transformation: (a) athermal; (b) burst; and (c) isothermal. After [13].

For the burst transformation mode (see Figure 1b), substantial transformation occurs in times less than about a millisecond when the temperature ( $M_s$  or  $M_b$ ) is reached on cooling. It is inferred that nucleation is inhibited and that significant undercooling below the equilibrium temperature ( $T_0$ ) produces a high chemical driving force that eventually triggers rapid auto-catalytic formation of martensite plates. Adiabatic heating can inhibit further transformation with burst kinetics and transformation then proceeds by either athermal or isothermal kinetics [13].

Isothermal kinetics (see Figure 1c) have been demonstrated in Fe-Ni and Fe-Ni-Mn alloys at subzero temperatures [13], with the time dependence of nucleation and growth being assumed to be due to the necessity for thermal fluctuations to assist movement of boundary dislocations. In athermal transformations, even at subzero temperatures, the chemical driving force is sufficiently large to effect rapid boundary motion without thermal activation.

The mechanism of nucleation of martensite has been intensively examined [5–8] and although it is generally acknowledged that transformation is initiated at dislocation sites in the austenite, the identity of the nucleus for a specific transformation is difficult to ascertain. One notable exception is the transformation of austenite to  $\epsilon$ -martensite in alloys with low stacking fault energy. In this case, the motion of Shockley partial dislocations on every second close-packed {111} plane of the austenite generates the close-packed hexagonal structure of the martensite [5,6].

### 3. Crystallography of the Martensitic Transformation

The major crystallographic features of the martensitic transformation are an orientation relationship between the two phases and a homogeneous shape strain with a specific interface plane. Theoretical predictions of these crystallographic features were achieved by Bowles and Mackenzie using a phenomenological theory developed in the period 1952–53 [15]. A similar theoretical approach was independently developed by Wechsler, Lieberman, and Read [16] during the same period.

Phenomenological theory allows the calculation of the observed geometric and crystallographic features of the transformation with the input of the lattice parameters, a lattice correspondence and an assumed internal shear system in the martensite.

#### 3.1. Homogeneous Shape Strain

One of the most striking features of the martensitic transformation is the surface relief associated with the plate-shaped product phase. This relief is often evident to the unaided eye and can be clearly observed by optical microscopy.

Since the specific volumes of the parent and product crystal structures are rarely the same, a volume change generally occurs on transformation. The surface relief accompanying formation of martensite plates is similar to that observed for deformation or mechanical twins and therefore a shear displacement is also inferred.

The characteristics of this surface relief indicate that the shape change accompanying martensitic transformation is a macroscopically homogeneous strain. This strain has been predicted theoretically [15] and confirmed experimentally [17–19] to be an invariant plane strain (IPS), with the habit or interface plane being the invariant plane. Using the nomenclature and the matrix formulation adopted by Bowles and Mackenzie [15],  $\mathbf{P}_1$ , the homogeneous shape strain is given by  $(\mathbf{I} + m_1 \mathbf{d}_1 \cdot \mathbf{p}_1')$ , where  $\mathbf{I}$  is the identity matrix,  $m_1$  is the magnitude of the IPS,  $\mathbf{d}_1$  is the direction of displacement (written as a  $[3 \times 1]$  matrix) and  $\mathbf{p}_1'$  is the normal to the invariant plane (a  $[1 \times 3]$  matrix).

Although experimental measurement of the elements of the shape strain is challenging, the validity of methods used have been confirmed by detailed analysis of twins produced in the body-centred tetragonal crystal structure of  $\beta$ -tin [20]. The experimental results conclusively demonstrated that the surface relief corresponds to a shear strain on the known twinning elements  $\{301\} \langle -1 \ 0 \ 3 \rangle$ .

Experimental measurement of the elements of the homogeneous shape strain provides an alternative means for estimating the volume change, by calculating the determinant of  $\mathbf{P}_1$ :

$$(1 + m_1 \cdot p_1' \cdot d_1)$$

This value can be compared with the calculated volume change ( $g$ ) obtained by measuring the lattice parameters of the two phases. The Bowles-Mackenzie (BM) theory assumes that the shape strain can deviate from an IPS by a small uniform distortion (a dilatation,  $\delta$ ) of the interface by up to about 1.5%. The dilatation can be estimated by the relationship

$$\delta = [(1 + m_1 \cdot p_1' \cdot d_1) / g]^{1/3} \quad (1)$$

It was common to regard any discrepancy between the measured and calculated volume change as proof that the actual homogeneous shape strain differed from an IPS by a uniform dilatation of the interface plane. This conclusion has since been disproven, at least for transformations in steels [18,21] and it is now widely accepted that the shape strain is an IPS. However, lack of exact agreement between  $g$  and the determinant of  $\mathbf{P}_1$  is sometimes reported [22] drawing attention to possible errors in measurements of the elements of the shape strain and/or the lattice parameters. This issue is discussed later.

The magnitude  $m_1$  of the IPS for steels is typically about 0.2 and if it is assumed that  $d_1$  lies at an angle of  $80^\circ$  from the habit plane normal  $p_1'$ , the shear component of the strain magnitude is 0.196 and the normal component (equivalent to the volume change) is 0.035. These typical figures demonstrate that the shear strain accompanying martensitic transformation is far more significant than the volumetric strain.

Martensitic transformation is obviously driven by the decrease in chemical free energy when the parent phase is replaced by the martensitic product phase. However, transformation is opposed by potentially significant increases in the surface and strain energies. Accommodation of interfacial and volumetric strains is therefore a key issue in determining the temperature range of transformation and, indeed, whether transformation is possible at all. If a change in magnetic state also occurs on transformation, magnetic energy is an additional factor to be considered in the energy balance. Consequently, externally applied magnetic and/or stress fields can then be used to influence transformation temperatures.

The relatively high shear strain characterizing thermally-induced martensitic transformation in steels and in other alloys can be compensated for by clustering of plates with opposing shear directions, leading to an overall shear strain that is close to zero for a group of self-accommodating plates [23,24]. This factor is reflected in habit planes that, although irrational, have close to two-fold symmetry in the parent crystal structure (e.g.,  $\{225\}_F$  in high carbon steel and  $\{331\}_B$  in Cu-based alloys). However, the volume change cannot be compensated for in polycrystalline alloys and for typical values in the range 2–4% for steels the volume change is likely to lead to plastic accommodation of the transformation by slip and/or twinning in the parent phase ahead of the growing plate. The resulting dislocations and/or mechanical twins are expected to be incorporated into the martensite, modifying the actual transformation strain. An effective counter to this problem is the analysis of single interface transformations in single crystals. Such experiments have been reported for Au-Cd [25] and In-Tl [26] alloys and provide uncomplicated data for the crystallography of the homogeneous shape strain.

Nevertheless, the formation of martensite in polycrystalline alloys is of far more practical importance and the means by which transformation strain is accommodated in this case is central to understanding the morphology and crystallography of the transformation. This challenge starts with analysis of the homogeneous shape strain produced by martensite plates intersecting the free surface of pre-polished samples. However, another cautionary note is appropriate as there is an implicit assumption that the strain manifest in plates intersecting the surface is the same as that resulting from transformation of fully embedded plates, which are subject to a different transformation-opposing environment. Moreover, there are several reports that indicate the martensite produced at the free surface can exhibit different transformation kinetics and crystallography compared to embedded or

bulk plates [27,28]. The same caveat applies to martensite formed in thin foils prepared for transmission electron microscopy [29].

### 3.2. Homogeneous Lattice Strain

The crystal structure change and the relative orientations of the parent and martensitic phases can also be described in terms of a homogeneous strain (the total lattice strain)  $\mathbf{S}$ . However, this strain is homogeneous only on an atomic or nanometric scale and is inconsistent with the macroscopic IPS. This apparent paradox has been resolved theoretically and confirmed experimentally by the observation of a lattice invariant shear (LIS),  $\mathbf{P}_2$  in the martensite [16,30]. The LIS can be in the form of internal twinning, stacking faults, or slip in the martensite [23] and it allows a macroscopically invariant interface (a plane of zero net distortion) to be established between the parent phase and the martensite.

The basic matrix equation of phenomenological theory, written with in terms of the total lattice strain is

$$\mathbf{S} = \mathbf{P}_1 \mathbf{P}_2 \quad (2)$$

or, expressed in terms of the homogeneous shape strain

$$\mathbf{P}_1 = \mathbf{S} \mathbf{P}_2^{-1} \quad (3)$$

The homogeneous lattice strain  $\mathbf{S}$  is defined in Equation (2) by two invariant plane strains and since the intersection of the two invariant planes must be an invariant line,  $\mathbf{S}$  can be described as an invariant line strain (ILS). It can also be resolved into a rotation  $\mathbf{R}$  which defines the orientation relationship between the two phases and  $\mathbf{B}$  which is the pure or Bain strain that results in the change in crystal structure

$$\mathbf{S} = \mathbf{R} \mathbf{B} \quad (4)$$

$\mathbf{B}$  generates the length changes consistent with the lattice strain  $\mathbf{S}$  and is characterized by the pure strains,  $\eta_i$  ( $i = 1$  to 3) which occur along orthogonal axes in the parent crystal structure corresponding to orthogonal axes of the martensite. In general, none of the  $\eta_i$  is unity, the condition required for  $\mathbf{S}$  to be an IPS. Therefore, periodic slip, faulting, or twinning is required to establish the invariant interface plane of the shape strain.

The phenomenological approach was not considered by Bowles and Mackenzie to be mechanistic (i.e., to describe the actual atom movements), but it does embody the principle of strain minimization and highlights the importance of accommodation effects involved in the transformation.

Although phenomenological theory has proven to be successful for predicting the crystallography of many transformations, there are some notable exceptions, particularly the  $\{225\}_F$  transformation in steels. In this case, a single lattice invariant shear does not account for the measured crystallographic properties and although double shear theories have been proposed [31,32] these have also been unsuccessful [33]. However, an ad hoc model for the  $\{225\}_F$  transformation: the plastic accommodation model [34], provides good agreement with most of the measured crystallographic features, but it requires the operation of multiple slip systems in the austenite ahead of a growing plate.

Discrepancies between measurements and predictions again draw attention to uncertainties in measured features of the transformation, particularly the lattice parameters, which are essential input data for theoretical predictions using phenomenological theory.

### 3.3. Errors and Variability in Measured Crystallographic Features

In the case of steels, the coefficient of thermal expansion/contraction for austenite (FCC) is about twice that for the body-centred cubic (BCC) crystal structure of ferrite and for martensite with either a BCC or body-centred tetragonal (BCT) crystal structure. This difference is apparent in the dilatometer trace of Figure 2, which is based on the austenite to lath martensite transformation in the Cr-bearing steel P91 (9 wt. % Cr, 1 wt. % Mo, and 0.1 wt. % C) [35]. The ratio of the lattice parameters of the two phases is not constant as the temperature changes and therefore the volume change and predicted crystallographic properties would be expected to vary with the temperature of formation of the martensite. The transformation volume change measured at  $M_f$  in this case is close to 2%, but this value will vary for

plates formed at different temperatures in the Ms–Mf range. The lattice parameters used for theoretical analysis are most commonly determined at room temperature from martensite and residual austenite. However, these parameters will not be those relevant to transformations occurring substantially above room temperature or at sub-zero temperatures. Therefore, it can be inferred that martensite plates formed at different temperatures in the transformation range will be characterized by progressively changing crystallographic features. It is common practice to study large well-defined plates that have formed at temperatures just below Ms and it is therefore likely that there will be a systematic error in using parameters measured at room temperature. This point is reinforced by sub-zero lattice parameter measurements reported for Fe<sub>3</sub>Pt alloys at different temperatures in the transformation range [36].

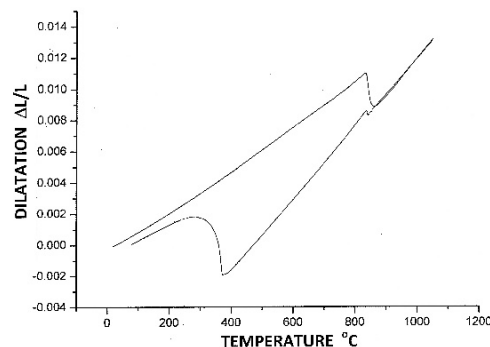


**Figure 2.** Dilatometer curves for a heating and cooling cycle for P91 steel. The length contraction at higher temperature corresponds to the formation of austenite and the expansion at lower temperatures signals the formation of martensite [35].

Habit plane measurements can be equally uncertain because plates are frequently curved rather than having well-defined parallel interfaces. The presence of thin plate martensite [37] or a mid-rib improves the accuracy with which the habit plane trace can be measured [38], but in many cases plates show significant curvature and there is considerable scatter in habit plane measurements due, at least in part, to variations in crystallography with the temperature of formation of the plate.

Scatter of habit plane measurements has been reported for both non-ferrous and ferrous alloys, with particular attention being focussed on iron-based alloys with notional  $\{225\}_F$ ,  $\{259\}_F$ , and  $\{3\ 10\ 15\}_F$  habit planes [39]. In 1957, Otte and Read concluded that a real scatter occurred, beyond their estimated measurement error of  $\pm 2^\circ$ , for habit planes measured in Fe–C–Cr alloy [40]. They proposed that deformation of the austenite resulting from the transformation volume change introduced constraints that affected the habit planes of subsequently formed plates. Another example is habit plane measurements in Fe–Ni alloys by Breedis and Wayman [38] which were based on average traces of curved surfaces of lenticular plates. Significant scatter was observed, which was reduced but not eliminated by using the more well-defined plate mid-rib. Bell and Bryans [41] also studied similar alloys using a two surface analysis technique with an estimated error of  $\pm 2^\circ$ . Although first formed plates in strain-free austenite had habit planes close to  $\{3\ 10\ 15\}_F$ , second and third generation plates varied significantly from  $\{3\ 10\ 15\}_F$ . They suggested that elastic and plastic strains introduced by prior transformation altered the invariant plane strain condition.

Christian [42] summarised these findings by concluding that the invariant plane strain condition might only be met for “unconstrained” single interface transformations. In polycrystalline austenite, local constraints could induce the operation of multiple and more complex lattice invariant shears, leading to significant habit plane variations.

However, there is a group of alloys for which the habit plane is rational and little or no scatter is observed. These alloys include Co and its dilute alloys, Fe–Mn–Si-based alloys and austenitic stainless steels. These alloys are characterized by low stacking fault energy for the FCC parent phase which can undergo transformation to  $\epsilon$ -martensite with a close packed hexagonal (CPH) crystal structure. The habit plane of the  $\epsilon$ -martensite is  $\{111\}_F$ .

Non-ferrous alloys can also display habit plane scatter, with a prominent example being  $\gamma_1'$  (2H) martensite plates formed from the  $\beta_1$  ordered BCC parent phase in Cu-Al-Ni alloys. Curved or undulating sections of the habit plane are common due to variations in the relative widths of the transformation twins [39], presumably because of adjustments during plate growth to accommodate localized stress fields. The twins are relatively coarse and have interface facet planes that can extend to form sub-plates. This observation indicates that the interface facet planes are planes of good atomic matching with the parent phase and can act as habit planes for plates that are not crystallographic variants of the main plate [39].

In the case of steels, the previously discussed variation in the lattice parameters with changing temperature is also likely to contribute to the observed variability in habit plane measurements because of the marked difference in thermal contraction for austenite and martensite (Figure 2).

Variation in the direction of the shape strain for  $(225)_F$  martensite over a range of about  $40^\circ$  parallel to the  $(111)_F$  plane has also been confirmed [18,22]. The origin of this flexibility is unclear, but is likely to be related to the crystallographic orientation of the surface exposed grain containing the martensite plate selected for shape strain measurement [18].

### 3.4. Accommodation of the Martensitic Transformation

Three kinds of accommodation effects have been identified by Dunne [43]. He defined the primary accommodation effect as the periodic twinning, slip (or faulting) that is an intrinsic part of the transformation mechanism and is based on the principle of minimising surface strain energy by establishing a macroscopically invariant interface plane between the martensite plate and the austenite. Secondary accommodation refers to second order atomic adjustments that are necessary on a fine scale in response to interfacial misfit strains. This type of accommodation can occur by elastic strain or by plastic strain through generation of misfit dislocations in the interfacial region. Tertiary accommodation applies to the shape change, which comprises bulk dilatational and shear displacements. Although the shear displacements can be compensated for by formation of multiple variant clusters of martensite plates, the volume change, if significant, must be accommodated by slip, twinning, or faulting in the austenite and/or the martensite.

## 4. Nature of the Parent–Martensite Interface

The habit plane is usually one of three types [42]:

- (a) Planar, irrational, and semi-coherent and separating a single crystal parent from a slipped or faulted single crystal of martensite;
- (b) Planar, irrational, and separating a single crystal parent from a twinned martensite product;
- (c) Curved and macroscopically displaced from the “true” (normally irrational) habit plane.

The interface is highly mobile during the forward transformation, propagating at about the speed of sound in the metal or alloy ( $\sim 1$  km/s) [42]. Interface motion is frequently described as being “glissile” or “frictionless”, with propagation involving (i) migration of planar sections of an interface composed of the termini of alternate twin related volumes; or (ii) migration of planar sections as a surface dislocation; or (iii) thickening by sweeping of consecutive steps across the interface.

Although the austenite–martensite interface is characterized by its capacity for rapid propagation to form martensite on cooling, reverse transformation to austenite by a similar rapid propagation process does not generally occur. Accommodation of transformational strains by plastic deformation, as discussed in Section 3.4, is usually so significant that interface locking occurs, preventing or retarding reverse motion of the interface on heating. In such cases, reversion of martensite to austenite can occur by diffusional transformation or by the nucleation of austenite platelets within martensite [44]. In carbon-bearing steels, decomposition by tempering can occur rapidly on reheating, with carbide pinning of martensite interfaces and eventual formation of austenite by diffusional means.

Nevertheless, re-transformation to austenite by reverse interface motion was discovered in 1949 by Kurdjumov and Khandros for a Cu-Al-Ni alloy [45]. This phenomenon was subsequently found in other alloys, including Au-Cd [46] and Ti-Ni alloys [47]. Kurdjumov and Khandros coined the term “thermoelastic transformation” to describe the “elastic” nature of the transformation—forward or reverse motion of the martensite/austenite interface with small changes in temperature or stress.

## 5. Reversible Martensitic Transformation

The thermoelastic behaviour in Cu-Al-Ni is associated with a small transformation hysteresis and involves a balance between stored elastic strain energy and the chemical free energy change. Hysteresis is normally measured by the difference between the temperature at which 50% austenite ( $T_{50A}$ ) occurs on heating and the temperature of 50% martensite formation on cooling ( $T_{50M}$ ). As these temperatures may be difficult to determine, the  $A_s$ ,  $A_f$ ,  $M_s$ , and  $M_f$  temperatures can be used to estimate the hysteresis [48]. Transformation hysteresis, however small, indicates that frictional resistance opposes the reverse motion of the interface, usually because of defects generated by the formation of the martensite.

For ordered  $Fe_3Pt$  alloy (1050 h at 550 °C), martensitic transformation is characterized by a small hysteresis (about 15 °C), see Figure 3d, and the transformation can be regarded as thermoelastic [11]. For the case of disordered austenite (Figure 3a), the martensite to austenite transformation does not occur by interface reversible motion and displays a hysteresis of about 450 °C [11].

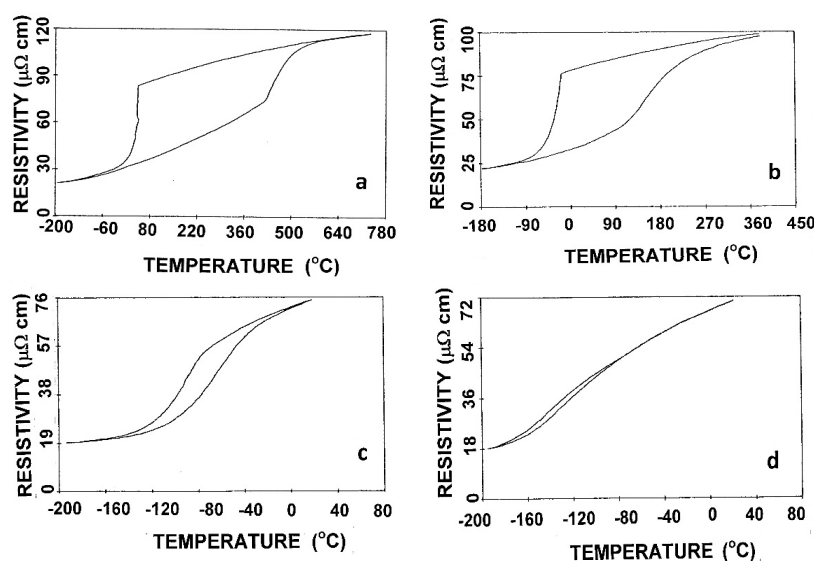


**Figure 3.** Resistivity versus temperature curves for the martensitic transformation in Fe-24 at. % Pt alloy: for disordered alloy (a); after ordering at 550 °C for 10 h (b); for 100 h (c); and for 1050 h (d). Note that the temperature and resistivity scales vary. After [11].

Progressive ordering of Fe-Pt alloy results in a full spectrum of mechanisms for reversion of martensite to austenite on heating. Partially ordered Fe-Pt alloys do show interface reversible transformation, but with a higher hysteresis than for highly ordered alloy. For example, Figure 3b is a plot of resistivity versus temperature for a sample ordered for 10 h at 550 °C which shows a hysteresis of about 180 °C; and Figure 3c, for a sample ordered for 100 h at 550 °C, displays a hysteresis of about 30 °C. These results indicate a trend away from burst transformation as order increases and the development of an increasing capacity for reversible interface motion to reform the austenite structure. For highly ordered alloy (Figure 3d), there is no indication of burst transformation and reverse transformation can occur readily with a small transformation hysteresis.

The effect of order on transformation temperatures for Fe-24 at. % Pt alloy is illustrated by Figure 4 which demonstrates the profound changes in  $M_s$ ,  $M_f$ ,  $A_s$ , and  $A_f$  [11]. The reverse transformation

temperatures,  $A_s$  and  $A_f$ , fall more rapidly with increasing order than  $M_s$  and  $M_f$ . Furthermore,  $A_s$  becomes significantly lower than  $M_s$  (see also, Figure 3d), indicating that stored elastic strain energy assists in driving the reverse transformation.

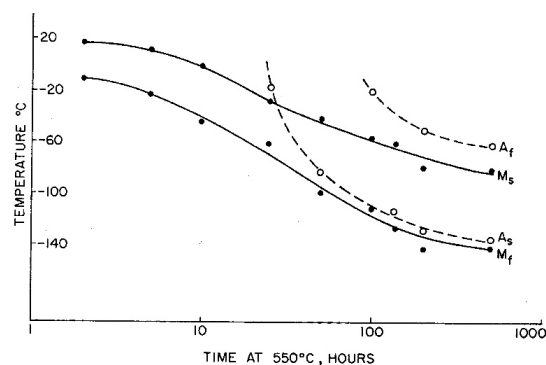


**Figure 4.** Transformation temperatures determined by direct observation during cold stage microscopy of Fe-24 at. %Pt alloy ordered for different times at 550 °C [11].

Confirmatory data are presented in Figure 5 for a 24.5 at. % Pt alloy ordered at the higher temperature of 650 °C. Ordering occurs over a much shorter time scale and the alloy is closer to the stoichiometric composition of Fe-25 at. %Pt for which it is possible to establish complete order ( $s = 1$ ). Transformation temperatures for this alloy were determined by DSC, which monitors changes in enthalpy during forward and reverse transformation. The trends in transformation temperatures are the same as those shown in Figure 4.

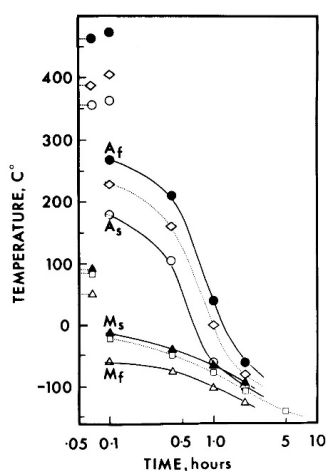


**Figure 5.** Transformation temperatures determined by DSC for Fe-24.5 at. %Pt alloy as a function of ordering time at 650 °C. The dotted lines show DSC peak temperatures and data points near the ordinate are for disordered alloy. Note that two reversion ranges are present after ordering for 0.1 h. [49].

Two other significant changes occur with increasing order, as demonstrated by Figure 6. The Curie temperature rises steeply with the onset of order and stabilizes at about 100 °C for well-ordered austenite. The ferromagnetic state stabilizes the austenite and contributes to the depression of  $M_s$ . Ordering also strongly affects the lattice parameter of the cubic austenite structure, increasing sharply from about 371.8 pm in disordered austenite to about 372.8 pm for substantially ordered austenite. Moreover, the lattice parameter shows little change with decreasing temperature in highly ordered samples, indicating the occurrence of Invar-type behaviour [36].

It is frequently stated that the overarching criterion for reversible thermoelastic martensitic phase transformation is the presence and maintenance of a glissile interface between martensite and

austenite, which implies frictionless interface motion in both the forward and reverse directions. However, this ideal state is effectively unachievable because the difference in crystal structures will, in general, lead to at least some atomic mismatch (misfit dislocations) in the interface. Even if mismatch can be largely accommodated by elastic strain, transformation hysteresis is invariably observed (see, for example, Figure 4d), indicating that there are interfacial defects that produce frictional resistance to interface motion. This reservation was taken into account by Olson and Cohen [50] who proposed that the relative absence of plastic accommodation of the shape strain is the single necessary and sufficient condition for thermoelastic transformation. However, the factors that allow this condition to be achieved have been the subject of considerable debate. On the basis of his studies of the development of interface reversible martensitic transformation with progressive ordering in Fe<sub>3</sub>Pt, Dunne [51] proposed that the important variables can be divided into those that limit the transformation strains and those that have the capacity to accommodate the transformation strains without the occurrence of irreversible deformation processes. The observed trends in transformation characteristics with increasing order in Fe<sub>3</sub>Pt are:

- Ms strongly decreases [11,49]
- the transformation hysteresis shrinks and the transformation becomes easily reversible [11]
- the martensite plates become much thinner [11]
- the Curie temperature rises (Figure 6) [49]
- the austenite exhibits Invar type behaviour [36,49]
- the martensite becomes BCT with a high tetragonality [36]
- the volume change becomes negligible (the shape strain approaches a shear) [36,51]
- the transformation twin spacing decreases [36]
- the austenite hardness increases (Figure 7) due to order hardening and magnetostriction [51,52]
- the habit plane normal shifts towards a plane of two-fold symmetry [51]
- elastic softening of the austenite crystal lattice occurs over a temperature range covering Ms, reducing the chemical driving force for nucleation [53].

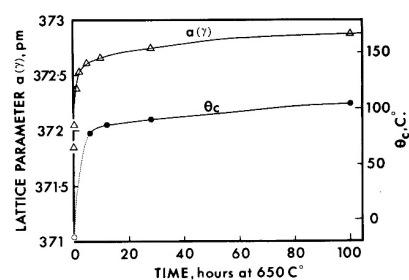


**Figure 6.** Graph showing changes in austenite lattice parameter and Curie temperature with ordering time at 650 °C for Fe-24.5 at. % Pt alloy [49].

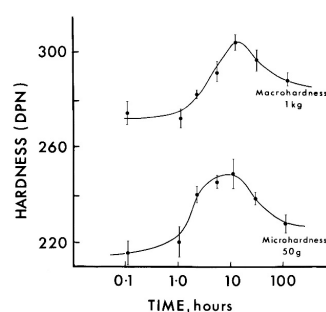


**Figure 7.** Variation in diamond pyramid hardness (1 kg and 50 g) with ordering time at 650 °C for Fe-24.5 at. % Pt alloy [51]. (Used with permission of The Minerals, Metals & Materials Society).

Table 1 summarises these characteristics and, although it is based on data for Fe-Pt, it is considered to reflect conditions that are relevant to the occurrence of crystallographically reversible martensitic transformation in all metals and alloys. A series of conditions must prevail that limit the magnitudes of the transformation strains and enhance the capacity of the alloy to effectively accommodate the transformation strains that do occur, without the occurrence of any significant irreversible plastic strain.

In the case of FePt the over-riding causative factor is increasing  $L1_2$  ordering of the face-centred cubic (FCC) austenite. The resulting factors given in Table 1 collectively provide a sufficient condition for thermoelastic reversible martensitic transformation. In effect, a “Goldilocks” zone is established which ensures that the martensite-austenite interface can move freely in both the forward and reverse directions.

Some of conditions in Table 1 may be necessary but are not sufficient *per se* to result in reversible transformation. For example, a volume change of close to zero in Fe-Ni-Co alloys [53,54] does not produce interface reversible transformation; nor does a habit plane close to {hhk} in Cu-Sn and Fe-C alloys and alloy steels. Furthermore, for some Cu-based alloys that show reversible transformation the LIS consists of regular faults in stacking rather than twinning [55].

**Table 1.** Factors contributing to reversible martensitic transformation in  $Fe_3Pt$ .

Strain Limiting Factor	Effect of Increasing Order
Low volume change	Volume change decreases [36]
Low magnitude of shape strain	$m_1$ decreases [51]
Low $\Delta G_c$	Shear modulus decreases [53]
Strain Accommodating Factor	Effect of Increasing Order
Thin plate morphology	Coarse lenticular plates replaced by thin plates [11]
High elastic limit for austenite	Yield stress and hardness increase due to magnetostrictive and order strengthening [51]
Self-accommodating plate groups	$p_1'$ approaches {hhk} <sub>F</sub> allowing the formation of self-accommodating four plate clusters [51]
Fine transformation twins	Twin boundary energy decreases with increase in martensite tetragonality [36,56,57]

## 6. Shape Memory Phenomena

Alloys capable of thermoelastic or interface reversible transformation are, in general, capable of exhibiting the property of shape memory.

The usual definition applied to a shape memory alloy is one that exhibits the capacity to “remember” and return to an original shape (S1) despite apparently permanent deformation to a significantly different shape (S2). If S1 is recovered completely and immediately on unloading, the effect can be described as pseudo-elasticity with the recovered strain being typically more than an order of magnitude higher than that at the normal elastic limit. Alternatively, if moderate heating is required to recover the shape S1, the alloy is exhibiting pseudo-plasticity. These two effects encompass and assist in rationalizing the range of shape memory phenomena reported in the literature and the variety in the nomenclature that has been used. Shape memory alloys have been assigned to various generalized classifications such as intelligent materials, smart materials, functional materials and ferroic materials. This identity confusion also extends to the names used to describe various shape memory phenomena: pseudoelasticity, superelasticity [23,24], shape memory effect [23,24], rubber-like effect [58], pseudoelasticity due to symmetry-conforming short range order (SC-SRO) of defects [59], intrinsic shape memory effect [60], one-way shape memory effect (OWSME), two-way shape memory effect (TWSME) [61], all-round shape memory effect (ARSME) [62], transformation-induced anelasticity [63], ferroelasticity [64], ferroplasticity [65].

The unifying characteristic of shape memory alloys is their capacity to undergo a crystallographically reversible martensitic phase change. There are however, only two basic shape memory phenomena: pseudo-elasticity (PE) and pseudo-plasticity (PP). PP and PE can be further sub-divided into effects that depend on the starting microstructural condition of the alloy. For example,

if the microstructure is completely or substantially martensitic at the temperature of “deformation” and the “undeformed” shape is completely or partially recovered by heating, the effect can be described as PP(M)—pseudo-plasticity associated with an initially martensitic microstructure. This behaviour indicates that the deformation step does not substantially involve irreversible plastic deformation by slip and/or mechanical twinning. Rather, the martensitic units present undergo reversible twinning or variant coalescence to accommodate the applied stress. On heating, these changes are reversed as transformation to the parent or austenite structure occurs over the temperature range  $A_s$  to  $A_f$ . In the usual case, subsequent cooling produces the undeformed martensitic condition, but cycling between the “deformed” and the initial shapes can be effected by thermal cycling after re-deforming the alloy in the cold state, for example by using a bias spring. It is also possible that cooling through the forward transformation range results in the martensite “remembering”, at least to some extent, its original “deformed” shape. This phenomenon has been called “two-way shape memory effect” and its origin lies in a residual stress bias in the reformed austenite grains that, on cooling, selects the martensite variants and their substructures produced by the initial deformation step. Such a stress bias is typically due to conventional plastic strain that accompanies the formation of the “deformed” martensitic structure. After reverse transformation, this plastic strain is inherited by the austenite in the form of residual dislocations that create an internal stress field [56]. Constrained aging can also promote two-way and all-round shape memory [62].

PP can also occur at temperatures above  $M_s$  for an original microstructure that is austenitic. Application of force can result in the formation of stress-induced martensite (SIM). The martensite variants activated produce a strain that accommodates the applied stress and subsequent heating to a temperature above  $A_f$  results in reversion of the stress-induced martensite to austenite with complete shape recovery. This effect can be termed PP(A). A similar overall effect can be obtained for a starting structure that is a mixture of austenite and martensite PP(M+A), but in this case accommodation of the applied stress can occur by formation of stress-induced martensite and/or twinning and variant coalescence of the pre-existing martensite. The starting microstructures and their relationship to the PP and PE effects are summarized in Table 2.

For the PE effect, the starting structure can again be martensite, a mixture of martensite and austenite, or austenite. PE does not require heating to recover the “deformed” shape, but simply requires removal of the “deforming” force. Stress cycling of pseudo-elastic Ti-Ni alloys can result in reproducible behaviour over thousands of cycles. The hysteresis involved in a complete stress–strain cycle is associated with absorption of energy—a characteristic that can be used for vibration damping under the influence of cyclic stresses.

**Table 2.** Proposed nomenclature for PP (pseudo-plastic) and PE (pseudo-elastic) shape memory phenomena.

Deformation Temperature $T_D$	PSEUDO—PLASTICITY		PSEUDO—ELASTICITY	
	Description	Recovery Temperature $T_R$	Description	Recovery Temperature $T_R$
$T_D < M_F$	PP(M)	$T_R > A_F$	PE(M)	$T_D$
$M_S < T_D < M_D$	PP(A)	$T_R > A_F$	PE(A)	$T_D$
$M_F < T_D < M_S$	PP(M+A)	$T_R > A_F$	PE(M+A)	$T_D$

Note:  $M_D$  is the maximum temperature for the formation of martensite by deformation.

The particular mechanisms by which these phenomena are exhibited will be a function of the alloy composition, the austenite grain size and substructure, the original thermal-mechanical condition of the austenite, the crystallographic relationship between the parent and martensite phases, the presence/absence of order or coherent precipitates, the effect of ageing treatment in the austenitic and/or martensitic state, and the type and magnitude of the deforming stress. In order to optimize the shape memory capacity of specific alloys a wide range of thermal, mechanical and thermal-mechanical

treatments has been investigated to change the texture, grain size, stacking fault density, dislocation density, and structure, or precipitate size and distribution in the austenite, prior to shape memory testing (see, for example, [62,66]).

Otsuka et al. [67] have attributed high importance to the crystallographic condition of a G-subG relationship which is based on the symmetry groups of the parent and martensite crystal structures [68]. Although this condition is significant in terms of the multiplicity of potential twinning modes in the martensite, and thus the capacity for both PE and PP and the magnitude of the recoverable strain, some alloys with G-subG relationships do not exhibit shape memory and others, despite the absence of a G-subG relationship, show at least limited shape memory behaviour.

One important aspect of shape memory behaviour is a reverse transformation path for the martensite that restores the original crystallographic orientation of the austenite. The martensite can potentially re-transform to austenite of different crystallographic variants, thereby negating shape recovery. For the case of ordered alloys, it is clear that the constraint imposed by the restoration of austenite order pre-determines the re-establishment of the original austenite orientation. Many shape memory alloys have an ordered parent phase and therefore it is obviously an important factor for the occurrence of crystallographically reversible martensitic transformation and shape memory. For shape memory alloys that are not ordered, such as FeNiCoTi [69] and more complex derivatives [70], heat-treatment can be used to produce fine coherent precipitates in the FCC austenite that result in the formation of BCT martensite with a high tetragonality [69]. The precipitates have been referred to as “memory units” that pre-determine the restoration of the original austenite orientation on stress release (PE) or heating (PP) [71]. Their effect on reverse transformation is therefore similar to that of atomic order.

It is perhaps less clear why stress-induced  $\epsilon$ -martensite reverts to the original austenite orientation on heating of Fe-Mn-Si-based shape memory alloys. However, this pathway is evidently the most energy-efficient way for reverse transformation to occur and it is likely that reversion is stress-field mediated as the mobile Shockley partial dislocations, which glide under stress along the  $\{111\}_F$  interface to produce the  $\epsilon$ -martensite plates, move in the reverse direction on heating, assisted by thermal activation, to recover the original austenite orientation.

Martensite is a transition phase that forms at relatively low temperatures because the kinetics of its formation reduces the free energy of the alloy more rapidly than competitive diffusional transformation to the equilibrium phases. Therefore, martensite is a metastable phase that is prone to diffusional decomposition during long term ageing or after multiple thermal cycles through the transformation range. Cu-based shape memory alloys are particularly susceptible to ageing effects and thermal cycling can result in drifting of transformation temperatures and even the elimination of martensitic transformation. Decomposition processes are particularly relevant to “high temperature” shape memory alloys based on Ti-Ni which include elements such as Zr, Hf, and Pd that serve to raise transformation temperatures [48]. Ti-Ni-based alloys designed to operate over lower and even sub-zero temperature are typically more stable, and pseudo-elastic alloys can sustain hundreds of thousands of stress cycles without fatigue failure, provided the maximum stress and strain values are restricted (typically, 1% recoverable strain and 70 MPa maximum stress [72]).

## 7. Conclusions

The early discoverers and investigators of the martensitic transformation could not have imagined the incredible bounty that could be, and has been, harvested by succeeding generations of scientists and engineers. In the case of ferrous martensite, a wide spectrum of sophisticated martensitic alloys has been developed and used to provide materials with ultra-high strength, outstanding toughness, wear resistance and creep resistance. Transformation-induced plasticity (TRIP) has been exploited for increasing ductility and toughness of alloy steels and shape memory steels have been developed. Similarly, many non-ferrous martensitic alloys have been developed with improved mechanical properties for engineering applications. In addition, advantage has been taken of shape memory

behaviour in Ti-Ni, Ti-Ni-based alloys, and Cu-based alloys to produce efficient connectors, thermal actuators, medical prostheses, and vibration damping devices.

Crystallography is less settled than is commonly assumed. Although phenomenological theory has been successful in accounting for observed crystallographic features of transformations characterized by a single lattice invariant shear, there are other cases where more complex multiple shears need to be invoked to account for observed crystallographic properties. Even so, no convincing general multiple shear theories have so far been developed. A further problem is that a fully martensitic alloy is likely to exhibit a spectrum of crystallographies because of the changing relationship between lattice parameters with temperature of formation, as well as the changing environment arising from austenite partitioning and transformation-induced elastic and plastic strains in the remaining austenite.

Nomenclature that has been previously used to describe the various shape memory effects tends to be both overlapping and confusing and a rationalized nomenclature is proposed that is based on the two fundamental observed phenomena: pseudo-elasticity and pseudo-plasticity.

The concept of the presence of a glissile interface as a single sufficient condition for crystallographically reversible martensitic transformation is unsatisfactory because interface motion cannot be frictionless. The necessary and sufficient condition proposed by Olson and Cohen: the relative absence of plastic accommodation of the shape strain, is more meaningful than a “glissile interface”, but the factors required to achieve this condition are unspecified. In the current paper, it is concluded that both strain limiting and strain accommodating conditions must be present and that for any particular alloy there will be multiple factors that together result in crystallographically reversible transformation. These factors collectively constitute the sufficient condition.

**Acknowledgments:** The author is indebted to a large number of research collaborators, postdoctoral researchers and PhD students over the course of his research career. In particular, the support and collaboration of John Bowles, Marvin Wayman, Noel Kennon, Hiro Otsuka, Jan Van Humbeeck, Huijun Li and Nicole Stanford are gratefully acknowledged.

**Conflicts of Interest:** The author declares that there are no conflicts of interest.

## References

1. Osmond, F. Nomenclature in Metallography. *J. Iron Steel Inst.* **1902**, *61*, 90.
2. Bain, E.C. *The Sorby Centennial Symposium on the History of Metallurgy*; Smith, C.S., Ed.; Gordon and Breach Science Publ.: New York, NY, USA, 1965.
3. Campbell, W. Twenty-Five Years of Metallography, 3rd Howe Memorial Award, 1926. *Trans. AIME* **1926**, *73*, 1135.
4. Greninger, A.B.; Mooradian, V.G. Strain transformation in metastable beta copper-zinc and beta copper-titanium alloys. *Trans. AIME* **1938**, *128*, 337.
5. Christian, J.W. Military Transformations: An Introductory Survey. In *Physical Properties of Martensite and Bainite*; Iron and Steel Institute: London, UK, 1965; p. 93.
6. Wayman, C.M. Martensitic Transformations. In *Modern Diffraction and Imaging Techniques in Materials Science*; Amelinckx, S., Gevers, R., Remaut, G., Van Landuyt, J., Eds.; North-Holland Publishing Company: Amsterdam, The Netherlands, 1970; pp. 187–232.
7. Olsen, G.B.; Owen, W.S. *Martensite*; ASM Press: Washington, DC, USA, 1992.
8. Petty, E.R. *Martensite*; Longman Group Ltd.: London, UK, 1970.
9. Nishiyama, Z. *Martensitic Transformations*; Academic Press: New York, NY, USA, 1978.
10. Bhattacharya, K. *Microstructure of Martensite: Why It Forms and How It Gives Rise to the Shape Memory Effect*; Oxford University Press: Oxford, UK, 2004.
11. Dunne, D.P.; Wayman, C.M. The effect of austenite ordering on the martensite transformation in Fe-Pt near the composition Fe<sub>3</sub>Pt: I. Morphology and transformation characteristics; II. Crystallography and general features. *Metall. Trans.* **1973**, *4*, 137–145. [[CrossRef](#)]
12. Wayman, C.M. On memory effects related to martensitic transformations and observations in  $\beta$  brass and Fe<sub>3</sub>Pt. *Scr. Metall.* **1971**, *5*, 489–492. [[CrossRef](#)]

13. Raghavan, V. Kinetics of martensitic transformation. In *Martensite*; Olsen, G.B., Owen, W.S., Eds.; ASM International: Cleveland, OH, USA, 1992; pp. 197–225.
14. Christian, J.W. Basic crystallography and kinetics. In *Martensite*; Petty, E.R., Ed.; Longman Group Ltd.: London, UK, 1970; Chapter 2; pp. 11–41.
15. Bowles, J.S.; Mackenzie, J. The crystallography of martensitic transformations I, II and III. *Acta Metall.* **1954**, *2*, 129–137, 138–147, 224–234. [[CrossRef](#)]
16. Wechsler, M.S.; Lieberman, D.S.; Read, T.A. On the theory of formation of martensite. *Trans. AIME* **1953**, *197*, 1503–1515.
17. Kennon, N.F.; Dunne, D.P. Shape strains associated with thermally-induced and stress-induced martensite in a Cu-Al-Ni shape memory alloy. *Acta Metall.* **1982**, *30*, 429–435. [[CrossRef](#)]
18. Dunne, D.P.; Bowles, J.S. Measurement of the shape strain for (225) and (259) martensitic transformations. *Acta Metall.* **1969**, *17*, 201–212. [[CrossRef](#)]
19. Efsic, E.J.; Wayman, C.M. Crystallography of the fcc-to-bcc martensitic transformation in an Fe-Pt alloy. *Trans. AIME* **1967**, *239*, 873–882.
20. Dunne, D.P.; Wayman, C.M. On the validity of methods for determining the shape strain in deformation twinning and martensitic transformations. *Acta Metall.* **1979**, *18*, 981–990. [[CrossRef](#)]
21. Krauklis, P.; Bowles, J.S. Direct measurement of the length change in the (225) martensite habit plane. *Acta Metall.* **1969**, *17*, 997. [[CrossRef](#)]
22. McDougall, P.G.; Wayman, C.M. The crystallography and morphology of ferrous martensites. In *Martensite*; Olsen, G.B., Owen, W.S., Eds.; ASM International: Cleveland, OH, USA, 1992; pp. 59–95.
23. Otsuka, K.; Wayman, C.M. Martensitic transformations: Crystallography. In *Shape Memory Materials*; Cambridge University Press: Cambridge, UK, 1998; pp. 5–21.
24. Otsuka, K.; Wayman, C.M. Mechanism of shape memory and superelasticity. In *Shape Memory Materials*; Cambridge University Press: Cambridge, UK, 1998; pp. 27–48.
25. Chang, L. On diffusionless transformation in Au-Cd single crystals containing 47.5 at. % Cd: Characterization of single interface transformation. *J. Appl. Phys.* **1952**, *23*, 725–728. [[CrossRef](#)]
26. Bazinski, Z.S.; Christian, J.W. Experiments on martensite transformation in single crystals of indium-thallium alloys. *Acta Metall.* **1954**, *2*, 148–166. [[CrossRef](#)]
27. Klostermann, J.A. The Concept of the Habit Plane and the Phenomenological Theories of the Martensite Transformation. *J. Less Common Met.* **1972**, *28*, 75–94. [[CrossRef](#)]
28. Umamoto, M.; Tamura, I. The morphology and substructure of butterfly martensite in ferrous alloys. *J. Phys. Colloq.* **1982**, *43*, C4-523–C4-528. [[CrossRef](#)]
29. Maki, T.; Wayman, C.M. Transmission electron microscope studies of thin foil martensite in Fe-Ni and Fe-Ni-C alloys. *Acta Metall.* **1977**, *25*, 681–693. [[CrossRef](#)]
30. Tamura, I.; Yoshimura, H.; Ibaraki, M.; Tagaya, M. Hardness and Structure of Ausformed Fe-Ni and Fe-Ni-C Alloys. *Trans. Jpn. Inst. Met.* **1964**, *5*, 47–52. [[CrossRef](#)]
31. Acton, A.F.; Bevis, M. A Generalized Martensite Crystallographic Theory. *Mater. Sci. Eng.* **1969**, *5*, 19. [[CrossRef](#)]
32. Ross, N.H.D.; Crocker, A.G. A generalized theory of the martensite crystallography and its application to transformations in steels. *Acta Metall.* **1970**, *18*, 405. [[CrossRef](#)]
33. Dunne, D.P.; Wayman, C.M. An assessment of the double shear theory as applied to ferrous martensitic transformations. *Acta Metall.* **1970**, *19*, 425–438. [[CrossRef](#)]
34. Bowles, J.S.; Dunne, D.P. The role of plastic accommodation in the (225) martensite transformation. *Acta Metall.* **1969**, *17*, 677–685. [[CrossRef](#)]
35. Sulaiman, S. Structure and Properties of the Heat Affected Zone of P91 Creep Resistant Steel. Ph.D. Thesis, University of Wollongong, Wollongong, Australia, July 2008.
36. Tadaki, T.; Shimizu, K. High tetragonality of the thermoelastic Fe<sub>3</sub>Pt martensite and small volume change during transformation. *Scr. Metall.* **1973**, *9*, 771–776. [[CrossRef](#)]
37. Maki, T.; Tamura, I. Shape memory effect in ferrous alloys. In *Proceedings of the International Conference on Martensitic Transformations, ICOMAT'86*; The Japan Institute of Metals: Sendai, Japan, 1987; pp. 963–970.
38. Breedis, J.F.; Wayman, C.M. The martensitic transformation in Fe-31 wt. % Ni. *Trans. AIME* **1962**, *24*, 1128–1133.

39. Dunne, D.; Kennon, N. The martensite interface—How regular is the habit? In Proceedings of the Interfaces II Conference, Melbourne, Australia, 2–5 June 1994; pp. 273–278.
40. Otte, H.M.; Read, T.A. Habit planes of martensite in chrome-carbon steel. *J. Met.* **1957**, *9*, 412–417. [[CrossRef](#)]
41. Bell, T.; Bryans, R.G. The Effect of Prior Transformation and Prestrain on the Habit Planes of Acicular Iron-Nickel Martensite. *Met. Sci. J.* **1971**, *5*, 135. [[CrossRef](#)]
42. Christian, J.W. *The Theory of Phase Transformations in Metals and Alloys*; Pergamon Press: Oxford, UK, 1965.
43. Dunne, D.P. The interface structure of martensite in Fe<sub>3</sub>Pt. *Scr. Metall.* **1978**, *12*, 143–146. [[CrossRef](#)]
44. Kessler, H.; Pitsch, W. On the nature of reverse martensite to austenite transformation. *Acta Metall.* **1967**, *15*, 401–405. [[CrossRef](#)]
45. Kurdjumov, G.V.; Khandros, L.G. On the “thermoelastic” equilibrium in martensitic transformations. *Dokl. Akad. Nauk SSSR* **1949**, *66*, 211–214. (In Russian)
46. Chang, L.C.; Read, T.A. Plastic Deformation and Diffusionless Phase Changes in Metals in the Gold-Cadmium Beta Phase. *Trans. AIME* **1951**, *191*, 47–52. [[CrossRef](#)]
47. Buehler, W.J.; Gilfrich, J.V.; Wiley, R.C. Effect of Low-Temperature Phase Changes on the Habit Planes of Alloys near the Composition TiNi. *J. Appl. Phys.* **1963**, *34*, 1475. [[CrossRef](#)]
48. Firstov, G.S.; Kosorukova, T.A.; Koval, Y.N.; Verhovlyuk, P.A. Directions for High-Temperature Shape Memory Alloy Improvement: Straight Way to High-Entropy Materials? *Shape Mem. Superelasticity* **2015**, *1*, 400–407. [[CrossRef](#)]
49. Dunne, D.P.; Stobbs, M.; Kennon, N.F. The effect of order on the martensitic transformation in Fe<sub>3</sub>Pt. *Proc. Mat. Res. Soc. Symp.* **1984**, *21*, 675–680. [[CrossRef](#)]
50. Olson, G.B.; Cohen, M. Reply to “On the equilibrium temperature and thermoelastic martensitic transformation”. *Scr. Metall.* **1977**, *11*, 345. [[CrossRef](#)]
51. Dunne, D.P. Martensitic iron-platinum alloys. In *Proceedings of the International Conference on Displacive Transformations and Their Applications in Materials Engineering*, Urbana, IL, USA; Inoue, K., Mukherjee, K., Otsuka, K., Chen, H., Eds.; TMS: Warrendale, PA, USA, 1996; pp. 133–140.
52. Davies, R.G.; Magee, C.L. Austenite ferromagnetism and martensite morphology. *Metall. Trans.* **1971**, *2*, 1939.
53. Grujicic, M.; Ling, H.C.; Haezebrouck, D.M.; Owen, W.S. Growth of martensite. In *Martensite*; Olsen, G.B., Owen, W.S., Eds.; ASM International: Cleveland, OH, USA, 1992; Chapter 10; pp. 175–197.
54. Magee, C.L.; Davies, R.G. On the volume expansion accompanying f.c.c. to b.c.c. transformation in ferrous alloys. *Acta Metall.* **1972**, *20*, 1031–1043. [[CrossRef](#)]
55. Lovey, F.C.; Van Tendeloo, G.; Van Lunduyt, J.; Delaey, L.; Amelinckx, S. On the nature of various stacking defects in 18R martensite in Cu-Al alloys. A study by high resolution microscopy. *Phys. Stat. Sol.* **1984**, *86*, 553–564. [[CrossRef](#)]
56. Kajiwara, S.; Owen, W.S. The reversible martensite transformation in iron-platinum alloys near Fe<sub>3</sub>Pt. *Metall. Trans.* **1974**, *5*, 2047–2061. [[CrossRef](#)]
57. Kajiwara, S.; Owen, W.S. The martensite-austenite interface and the thickness of twins in Fe<sub>3</sub>Pt. *Scr. Metall.* **1977**, *11*, 137–142. [[CrossRef](#)]
58. Otsuka, K.; Wayman, C.M. Introduction. In *Shape Memory Materials*; Cambridge University Press: Cambridge, UK, 1998; pp. 1–26.
59. Ren, X.; Otsuka, K. Origin of rubber-like behaviour in metal alloys. *Nature* **1997**, *389*, 579–582.
60. Otsuka, K.; (NRIM, Tsukuba Japan). Personal communication, 2011.
61. Saburi, T. Ti-Ni shape memory alloys. In *Shape Memory Materials*; Otsuka, K., Wayman, C.M., Eds.; Cambridge University Press: Cambridge, UK, 1998; pp. 49–96.
62. Nishida, M.; Honma, T. All-round shape memory effect in Ni-rich TiNi alloys generated by constrained aging. *Scr. Metall.* **1984**, *18*, 1293. [[CrossRef](#)]
63. Dunne, D.P. Transformation-induced anelasticity. *J. Aust. Inst. Met.* **1974**, *19*, 28–34.
64. Lieberman, D.S. *Phase Transformations*; ASM: Geauga County, OH, USA, 1970; Volume 1.
65. Lieberman, D.S.; Schmerling, M.A.; Karz, R.W. Ferroelastic ‘memory’ and mechanical properties of gold-cadmium. In *Shape Memory Effects in Alloys*; Perkins, J., Ed.; Plenum Press: New York, NY, USA, 1975; pp. 203–244.
66. Stalmans, R.; Van Humbeeck, J.; Delaey, L. Training of copper based shape memory alloys. In Proceedings of the ICOMAT—92, Monterey, CA, USA, 20–24 July 1993; pp. 1065–1070.

67. Otsuka, K.; Saxena, A.; Deng, J.; Ren, X. Mechanism of the shape memory effect in martensitic alloys: An assessment. *Philos. Mag.* **2011**, *91*, 4514–4535. [[CrossRef](#)]
68. Bhattacharya, K.; Conti, S.; Zanzotto, G.; Zimmer, J. Crystal symmetry and the reversibility of martensitic transformations. *Nature* **2004**, *428*, 55. [[CrossRef](#)] [[PubMed](#)]
69. Maki, T. Microstructure and mechanical behaviour of ferrous martensite. In *Proceedings of the International Conference on Martensitic Transformations (ICOMAT'89)*; Materials Science Forum; Muddle, B.C., Ed.; Trans Tech Publications Ltd: Stafa-Zurich, Switzerland, 1990; Volume 56–58, pp. 157–168.
70. Ohmori, T.; Ando, K.; Okana, M.; Xu, X.; Tanaka, Y.; Ohnuma, I.; Kainuma, R.; Ishida, K. Superelastic Effect in Polycrystalline Ferrous Alloys. *Science* **2011**, *333*, 68. [[CrossRef](#)] [[PubMed](#)]
71. Koval, Y.N.; Monastyrsky, G.E. Reversible martensite transformation and shape memory effect in Fe-Ni-Nb alloys. *Scr. Metall.* **1993**, *28*, 41–48. [[CrossRef](#)]
72. Stockel, D. *Status and Trends in Shape Memory Technology*; Nitinol Development Corporation: Pittsburgh, PA, USA, 1992; pp. 79–84.



© 2018 by the author. Licensee MDPI, Basel, Switzerland. This article is an open access article distributed under the terms and conditions of the Creative Commons Attribution (CC BY) license (<http://creativecommons.org/licenses/by/4.0/>).